

Two rigid non-circular inhomogeneities in an elastic matrix

X. WANG¹⁾, P. SCHIAVONE²⁾

¹⁾*School of Mechanical and Power Engineering, East China University of Science and Technology, 130 Meilong Road, Shanghai 200237, China, e-mail: xuwang@ecust.edu.cn*

²⁾*Department of Mechanical Engineering, University of Alberta, 10-203 Donadeo Innovation Centre for Engineering, Edmonton, Alberta, T6G 1H9 Canada, e-mail: p.schiavone@ualberta.ca*

WE DERIVE ANALYTICAL SOLUTIONS TO THE PLANE ELASTICITY PROBLEM of two interacting identical rigid non-circular inhomogeneities embedded in an infinite isotropic elastic matrix subjected to uniform remote in-plane normal and shear stresses. Explicit expressions for the pair of analytic functions due to remote normal and shear stresses are obtained with the aid of analytic continuation and a conformal mapping function for the doubly connected quadrature domain occupied by the matrix. The rigid body rotation of each rigid inhomogeneity induced by a uniform remote shear stress is determined once three corresponding regular integrals are evaluated. The remote asymptotic behaviors of the pair of analytic functions are determined once five associated regular integrals are evaluated.

Key words: two rigid non-circular rigid inhomogeneities, quadrature domain, conformal mapping, analytic continuation, rigid body rotation, analytical solution.



Copyright © 2025 The Authors.

Published by IPPT PAN. This is an open access article under the Creative Commons Attribution License CC BY 4.0 (<https://creativecommons.org/licenses/by/4.0/>).

1. Introduction

STRESS ANALYSIS IN PLANE ELASTICITY can be accomplished with the aid of the techniques of conformal mapping [1] and analytic continuation [2]. The analysis becomes formidably challenging when the domain occupied by the elastic body is multiply connected, for example an infinite elastic plane containing multiple interacting pores or multiple interacting rigid inhomogeneities. CROWDY [3] introduced a conformal mapping function for quadrature domains to solve the plane elasticity problem of an infinite elastic plane containing two interacting equal symmetric pores. The pair of analytic functions characterizing the stress field in the elastic body can be written explicitly in terms of the Schottky–Klein prime function. Crowdy’s method has been recently applied by WANG and SCHIAVONE [4] to study two interacting identical non-circular compressible liquid inclusions embedded in an infinite isotropic elastic matrix subjected to uniform remote in-plane stresses.

In this paper we continue our recent accomplishments in this direction and study the plane elasticity problem associated with two interacting equal symmetric rigid inhomogeneities embedded in an infinite isotropic elastic matrix subjected to uniform remote in-plane normal and shear stresses. Through the introduction of a conformal mapping function for the doubly connected quadrature domain occupied by the matrix [3] and analytic continuation [2], the pair of analytic functions can be expressed explicitly in terms of the Schottky–Klein prime function. Analytical solutions for the two loading cases of uniform remote normal stresses and a uniform remote shear stress are derived. In particular, the rigid body rotation of each rigid inhomogeneity induced by remote shear stress is obtained by imposing the condition of balance of moments around each rigid inhomogeneity. The three regular integrals appearing in the expression for rigid body rotation are evaluated by the trapezoidal rule [3]. The remote asymptotic behaviors of the pair of analytic functions are determined once the five corresponding regular integrals are evaluated. Numerical results for the rigid body rotation of each rigid inhomogeneity and the remote asymptotic behaviors of the pair of analytic functions are presented. When the conformal modulus in the conformal mapping function approaches zero and unity, the rigid body rotation of each rigid inhomogeneity and remote behaviors of the pair of analytic functions are in agreement with available results for an isolated rigid elliptical or circular inhomogeneity [5–8].

2. Muskhelishvili's complex variable formulation

A Cartesian coordinate system $\{x_i\}$ ($i = 1, 2, 3$) is established. For the in-plane deformations of an isotropic elastic material, the three in-plane stresses $(\sigma_{11}, \sigma_{22}, \sigma_{12})$, two in-plane displacements (u_1, u_2) and two stress functions (φ_1, φ_2) are given in terms of two analytic functions $\phi(z)$ and $\psi(z)$ of the complex variable $z = x_1 + ix_2$ as [1]:

$$(2.1) \quad \begin{aligned} \sigma_{11} + \sigma_{22} &= 2[\phi'(z) + \overline{\phi'(z)}], \\ \sigma_{22} - \sigma_{11} + 2i\sigma_{12} &= 2[\bar{z}\phi''(z) + \psi'(z)], \end{aligned}$$

and

$$(2.2) \quad \begin{aligned} 2\mu(u_1 + iu_2) &= \kappa\phi(z) - z\overline{\phi'(z)} - \overline{\psi(z)}, \\ \varphi_1 + i\varphi_2 &= i[\phi(z) + z\overline{\phi'(z)} + \overline{\psi(z)}], \end{aligned}$$

where $\kappa = 3 - 4\nu$ for plane strain and $\kappa = (3 - \nu)/(1 + \nu)$ for plane stress, μ and ν ($0 \leq \nu \leq 1/2$) are the shear modulus and Poisson's ratio, respectively. In addition, the stresses are related to the two stress functions through [9]:

$$(2.3) \quad \begin{aligned} \sigma_{11} &= -\varphi_{1,2}, & \sigma_{12} &= \varphi_{1,1}, \\ \sigma_{21} &= -\varphi_{2,2}, & \sigma_{22} &= \varphi_{2,1}. \end{aligned}$$

3. Preliminary

As shown in Fig. 1, we consider two equal symmetric rigid non-circular inhomogeneities embedded in an infinite isotropic elastic matrix subjected to uniform remote in-plane normal and shear stresses $(\sigma_{11}^\infty, \sigma_{22}^\infty, \sigma_{12}^\infty)$. The two rigid inhomogeneities are perfectly bonded to the matrix through the left and right inhomogeneity-matrix interfaces L_1 and L_2 . The rigid body rotation at infinity is zero.

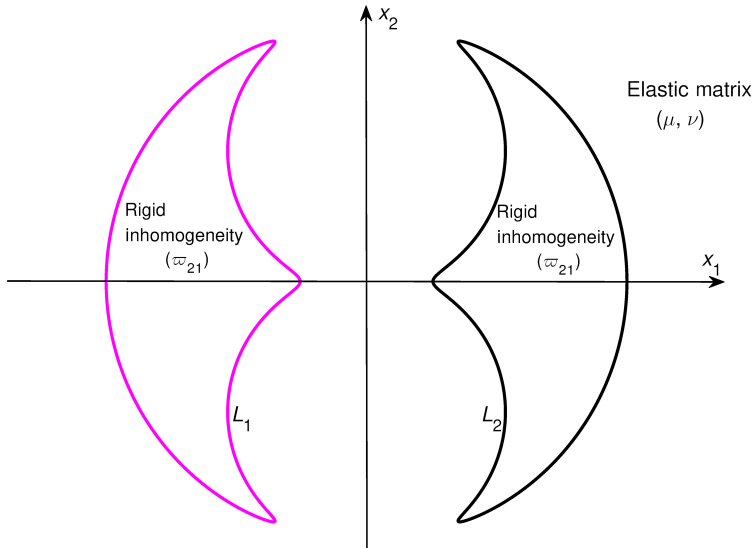


FIG. 1. Two equal symmetric rigid non-circular inhomogeneities embedded in an infinite isotropic elastic matrix subjected to uniform remote in-plane normal and shear stresses.

We introduce the following conformal mapping function for the matrix [3]:

$$(3.1) \quad z = \omega(\xi) = R \frac{P(-\xi\sqrt{\rho})P(-\xi\sqrt{\rho})P(\xi\sqrt{\rho})}{P(\xi\sqrt{\rho})P(\xi\sqrt{\rho}e^{i\theta})P(\xi\sqrt{\rho}e^{-i\theta})}, \quad \rho \leq |\xi| \leq 1,$$

where R , θ and the conformal modulus ρ governing the interaction of the two rigid inhomogeneities are real constants, and

$$(3.2) \quad P(\xi) = (1 - \xi)\hat{P}(\xi), \quad \hat{P}(\xi) = \prod_{k=1}^{+\infty} (1 - \rho^{2k}\xi)(1 - \rho^{2k}\xi^{-1}).$$

As shown in Fig. 2, using the mapping function in Eq. (3.1), the doubly connected quadrature domain occupied by the matrix is mapped onto the annulus $\rho \leq |\xi| \leq 1$; the left inhomogeneity-matrix interface L_1 is mapped onto the unit circle $|\xi| = 1$ and the right inhomogeneity-matrix interface L_2 is mapped onto the inner concentric circle $|\xi| = \rho$; the point $z = \infty$ is mapped onto $\xi = \sqrt{\rho}$ and the point $z = 0$ is mapped onto $\xi = -\sqrt{\rho}$.

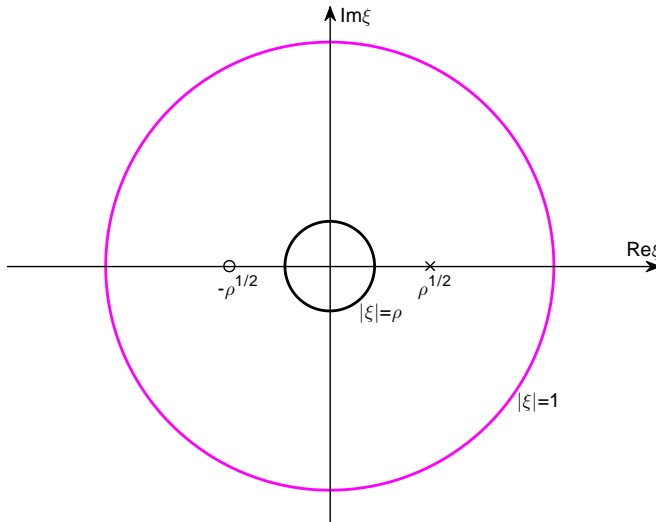


FIG. 2. The image ξ -plane.

The continuity of displacements across the two perfect interfaces L_1 and L_2 can be expressed in terms of the pair of analytic functions $\phi(z)$ and $\psi(z)$ defined in the matrix as:

$$(3.3) \quad \begin{aligned} \kappa\phi(z) - z\overline{\phi'(z)} - \overline{\psi(z)} &= 2i\mu\varpi_{21}z + \gamma, & z \in L_1, \\ \kappa\phi(z) - z\overline{\phi'(z)} - \overline{\psi(z)} &= 2i\mu\varpi_{21}z - \gamma, & z \in L_2, \end{aligned}$$

where $\varpi_{21} = \frac{1}{2}(u_{2,1} - u_{1,2})$ is the unknown rigid body rotation of each rigid inhomogeneity and γ is an unknown complex constant.

The pair of analytic functions $\phi(z)$ and $\psi(z)$ can be written in the following form:

$$(3.4) \quad \begin{aligned} \phi(z) &= \phi_1(z) + \frac{\sigma_{11}^\infty + \sigma_{22}^\infty}{4}z, \\ \psi(z) &= \psi_1(z) + \frac{\sigma_{22}^\infty - \sigma_{11}^\infty + 2i\sigma_{12}^\infty}{2}z, \end{aligned}$$

where $\phi_1(z) \cong O(1)$, $\psi_1(z) \cong O(1)$ as $|z| \rightarrow \infty$. Thus $\phi_1(z)$ and $\psi_1(z)$ are the perturbed parts of $\phi(z)$ and $\psi(z)$ due to the presence of the two rigid inhomogeneities.

Substitution of Eq. (3.4) into Eq. (3.3) yields:

$$\begin{aligned}
 & \kappa\phi_1(z) - z\overline{\phi_1'(z)} - \overline{\psi_1(z)} \\
 &= \left[2i\mu\varpi_{21} - \frac{(\kappa-1)(\sigma_{11}^\infty + \sigma_{22}^\infty)}{4} \right] z + \frac{\sigma_{22}^\infty - \sigma_{11}^\infty - 2i\sigma_{12}^\infty}{2} \bar{z} + \gamma, \quad z \in L_1, \\
 & \kappa\phi_1(z) - z\overline{\phi_1'(z)} - \overline{\psi_1(z)} \\
 &= \left[2i\mu\varpi_{21} - \frac{(\kappa-1)(\sigma_{11}^\infty + \sigma_{22}^\infty)}{4} \right] z + \frac{\sigma_{22}^\infty - \sigma_{11}^\infty - 2i\sigma_{12}^\infty}{2} \bar{z} - \gamma, \quad z \in L_2.
 \end{aligned}
 \tag{3.5}$$

Considering the mapping function in Eq. (3.1), the interface conditions in Eq. (3.5) can be expressed in the ξ -plane as:

$$\begin{aligned}
 & \kappa\bar{\phi}_1\left(\frac{1}{\xi}\right) - \bar{\omega}\left(\frac{1}{\xi}\right) \frac{\phi_1'(\xi)}{\omega'(\xi)} - \psi_1(\xi) \\
 &= -\left[2i\mu\varpi_{21} + \frac{(\kappa-1)(\sigma_{11}^\infty + \sigma_{22}^\infty)}{4} \right] \bar{\omega}\left(\frac{1}{\xi}\right) \\
 &\quad + \frac{\sigma_{22}^\infty - \sigma_{11}^\infty + 2i\sigma_{12}^\infty}{2} \omega(\xi) + \bar{\gamma}, \quad |\xi| = 1, \\
 & \kappa\bar{\phi}_1\left(\frac{\rho^2}{\xi}\right) - \bar{\omega}\left(\frac{\rho^2}{\xi}\right) \frac{\phi_1'(\xi)}{\omega'(\xi)} - \psi_1(\xi) \\
 &= -\left[2i\mu\varpi_{21} + \frac{(\kappa-1)(\sigma_{11}^\infty + \sigma_{22}^\infty)}{4} \right] \bar{\omega}\left(\frac{\rho^2}{\xi}\right) \\
 &\quad + \frac{\sigma_{22}^\infty - \sigma_{11}^\infty + 2i\sigma_{12}^\infty}{2} \omega(\xi) - \bar{\gamma}, \quad |\xi| = \rho,
 \end{aligned}
 \tag{3.6}$$

where for convenience we write $\phi_1(\xi) = \phi_1(\omega(\xi))$ and $\psi_1(\xi) = \psi_1(\omega(\xi))$. The technique of analytic continuation [2] has been applied in writing Eq. (3.6).

Subtracting the two conditions in Eq. (3.6) and making use of the following property for quadrature domains [3]:

$$\bar{\omega}\left(\frac{\rho^2}{\xi}\right) = \bar{\omega}\left(\frac{1}{\xi}\right),
 \tag{3.7}$$

we arrive at

$$\bar{\phi}_1\left(\frac{\rho^2}{\xi}\right) - \bar{\phi}_1\left(\frac{1}{\xi}\right) = -\frac{2\bar{\gamma}}{\kappa},
 \tag{3.8}$$

or equivalently

$$\phi_1(\rho^2\xi) - \phi_1(\xi) = -\frac{2\gamma}{\kappa}.
 \tag{3.9}$$

It follows from Eq. (3.6)₁ that

$$(3.10) \quad \kappa\phi_1(\xi) = \left[2i\mu\varpi_{21} - \frac{(\kappa-1)(\sigma_{11}^\infty + \sigma_{22}^\infty)}{4} \right] \omega(\xi) \\ + \frac{\sigma_{22}^\infty - \sigma_{11}^\infty - 2i\sigma_{12}^\infty}{2} \bar{\omega}\left(\frac{1}{\xi}\right) + \omega(\xi) \frac{\bar{\phi}'_1\left(\frac{1}{\xi}\right)}{\bar{\omega}'\left(\frac{1}{\xi}\right)} + \bar{\psi}_1\left(\frac{1}{\xi}\right) + \gamma,$$

which serves as an analytic continuation of $\phi_1(\xi)$ across $|\xi| = 1$.

In the ensuing two sections, mainly with the aid of the conformal mapping in Eq. (3.1) and the analytic continuation in Eq. (3.10), we derive analytical solutions for the two loading cases of uniform remote normal stresses with $\sigma_{12}^\infty = 0$ and a uniform remote shear stress with $\sigma_{11}^\infty = \sigma_{22}^\infty = 0$, respectively in view of the fact that the solution structures for the two loading cases are different.

4. Remote normal stresses ($\sigma_{12}^\infty = 0$)

When the matrix is subjected to uniform remote normal stresses σ_{11}^∞ and σ_{22}^∞ , we have $\varpi_{21} = 0$. Considering Eq. (3.10) with $\sigma_{12}^\infty = 0$ and $\varpi_{21} = 0$, the analytic function $\phi_1(\xi)$ takes the form:

$$(4.1) \quad \phi_1(\xi) = -\frac{(\kappa-1)(\sigma_{11}^\infty + \sigma_{22}^\infty)}{4} [AK(\xi\sqrt{\rho}e^{i\theta}) + BK(\xi\sqrt{\rho}e^{-i\theta})] \\ + \frac{\sigma_{11}^\infty - \sigma_{22}^\infty}{2} [CK(\xi\sqrt{\rho}) + DK(\xi\sqrt{\rho}e^{i\theta}) + EK(\xi\sqrt{\rho}e^{-i\theta})] + F, \quad \rho \leq |\xi| \leq \frac{1}{\rho},$$

where A, B, C, D, E , and F are unknown complex constants to be determined, and

$$(4.2) \quad K(\xi) = \frac{\xi P'(\xi)}{P(\xi)} = -\frac{\xi}{1-\xi} + \sum_{n=1}^{+\infty} \left(-\frac{\rho^{2n}\xi}{1-\rho^{2n}\xi} + \frac{\rho^{2n}/\xi}{1-\rho^{2n}/\xi} \right).$$

Substituting Eq. (4.1) into Eq. (3.10) and equating the residues of the three simple poles at $\xi = e^{\pm i\theta}/\sqrt{\rho}$, $1/\sqrt{\rho}$, we obtain:

$$(4.3) \quad A = B = -\frac{1}{\frac{L(\rho) + L(\rho e^{-2i\theta})}{X} - \frac{\kappa e^{i\theta}}{\sqrt{\rho a}}}, \\ C = -\frac{\sqrt{\rho}b}{\kappa}, \quad D = E = \frac{CL(\rho e^{-i\theta})}{X}A,$$

where

$$\begin{aligned}
 L(\xi) &= \xi \frac{dK(\xi)}{d\xi} = - \sum_{n=0}^{+\infty} \frac{\rho^{2n}\xi}{(1 - \rho^{2n}/\xi)^2} - \sum_{n=1}^{+\infty} \frac{\rho^{2n}/\xi}{(1 - \rho^{2n}/\xi)^2}, \\
 a &= - \frac{R}{\sqrt{\rho}e^{i\theta}} \frac{P(-e^{-i\theta}/\rho)P(e^{-i\theta})P(-e^{-i\theta})}{\hat{P}(1)P(e^{-i\theta}/\rho)P(e^{-2i\theta})}, \\
 (4.4) \quad b &= \frac{RP(-1)P(-\rho)P(\rho)}{\sqrt{\rho}\hat{P}(1)P(\rho e^{i\theta})P(\rho e^{-i\theta})}, \\
 X = \bar{X} &= \frac{RP(-e^{i\theta})P(\rho e^{i\theta})P(-\rho e^{i\theta})}{P(e^{i\theta})P(\rho e^{2i\theta})P(\rho)} \\
 &\quad \times [K(-e^{i\theta}) + K(\rho e^{i\theta}) + K(-\rho e^{i\theta}) - K(e^{i\theta}) - K(\rho e^{2i\theta}) - K(\rho)].
 \end{aligned}$$

It is seen from Eq. (4.3) that the five constants A , B , C , D , and E are in fact real valued. In view of Eq. (4.3), we can rewrite Eq. (4.1) in the following form

$$\begin{aligned}
 (4.5) \quad \phi_1(\xi) &= A \left[- \frac{(\kappa - 1)(\sigma_{11}^\infty + \sigma_{22}^\infty)}{4} + \frac{CL(\rho e^{-i\theta})(\sigma_{11}^\infty - \sigma_{22}^\infty)}{2X} \right] \\
 &\quad \times [K(\xi\sqrt{\rho}e^{i\theta}) + K(\xi\sqrt{\rho}e^{-i\theta})] \\
 &\quad + \frac{C(\sigma_{11}^\infty - \sigma_{22}^\infty)}{2} K(\xi\sqrt{\rho}) + F, \quad \rho \leq |\xi| \leq \frac{1}{\rho}.
 \end{aligned}$$

Substituting Eq. (4.5) into Eq. (3.9) and using the following property [3]

$$(4.6) \quad K(\rho^2\xi) = K(\xi) - 1,$$

we arrive at the constant γ as follows

$$(4.7) \quad \gamma = \frac{\kappa A}{4} \left[-(\kappa - 1)(\sigma_{11}^\infty + \sigma_{22}^\infty) + \frac{2CL(\rho e^{-i\theta})(\sigma_{11}^\infty - \sigma_{22}^\infty)}{X} \right] + \frac{\kappa C(\sigma_{11}^\infty - \sigma_{22}^\infty)}{4},$$

which indicates that γ is real valued.

Using Eq. (4.5) to enforce the following condition that

$$(4.8) \quad \phi_1(z)|_{z=0} = \phi_1(\xi)|_{\xi=-\sqrt{\rho}} = 0,$$

we arrive at the constant F :

$$\begin{aligned}
 (4.9) \quad F &= -A \left[- \frac{(\kappa - 1)(\sigma_{11}^\infty + \sigma_{22}^\infty)}{4} + \frac{CL(\rho e^{-i\theta})(\sigma_{11}^\infty - \sigma_{22}^\infty)}{2X} \right] \\
 &\quad \times [K(-\rho e^{i\theta}) + K(-\rho e^{-i\theta})] - \frac{C(\sigma_{11}^\infty - \sigma_{22}^\infty)}{2} K(-\rho) \\
 &= \frac{C(\sigma_{22}^\infty - \sigma_{11}^\infty)}{2} K(-\rho),
 \end{aligned}$$

which indicates that the constant F is also real valued.

Now the analytic function $\phi_1(\xi)$ has been completely determined. The other analytic function $\psi_1(\xi)$ can be obtained from the analytic continuation in Eq. (3.10) as

$$(4.10) \quad \begin{aligned} \psi_1(\xi) = & \frac{(\kappa - 1)(\sigma_{11}^\infty + \sigma_{22}^\infty)}{4} \bar{\omega}\left(\frac{1}{\xi}\right) + \frac{\sigma_{11}^\infty - \sigma_{22}^\infty}{2} \omega(\xi) \\ & + \kappa \bar{\phi}_1\left(\frac{1}{\xi}\right) - \bar{\omega}\left(\frac{1}{\xi}\right) \frac{\phi_1'(\xi)}{\omega'(\xi)} - \gamma, \quad \rho \leq |\xi| \leq 1. \end{aligned}$$

Substituting $\phi_1(\xi)$ and $\psi_1(\xi)$ obtained above into Eq. (3.4) and then the resulting expressions into Eqs. (2.1) and (2.2), we arrive at the elastic field of stresses and displacements in the matrix due to uniform remote normal stresses σ_{11}^∞ and σ_{22}^∞ .

5. Remote shear stress ($\sigma_{11}^\infty = \sigma_{22}^\infty = 0$)

Considering Eq. (3.10) with $\sigma_{11}^\infty = \sigma_{22}^\infty = 0$, $\phi_1(\xi)$ takes the form:

$$(5.1) \quad \begin{aligned} \phi_1(\xi) = & 2i\mu\varpi_{21} [AK(\xi\sqrt{\rho}e^{i\theta}) + BK(\xi\sqrt{\rho}e^{-i\theta})] \\ & + i\sigma_{12}^\infty [CK(\xi\sqrt{\rho}) + DK(\xi\sqrt{\rho}e^{i\theta}) + EK(\xi\sqrt{\rho}e^{-i\theta})] + F, \quad \rho \leq |\xi| \leq \frac{1}{\rho}, \end{aligned}$$

where A, B, C, D, E , and F are unknown complex constants to be determined.

Substituting Eq. (5.1) into Eq. (3.10) and equating the residues of the three simple poles at $\xi = e^{\pm i\theta}/\sqrt{\rho}$, $1/\sqrt{\rho}$, we obtain:

$$(5.2) \quad \begin{aligned} A = B = & \frac{1}{\frac{L(\rho) + L(\rho e^{-2i\theta})}{X} + \frac{\kappa e^{i\theta}}{\sqrt{\rho a}}}, \\ C = & -\frac{\sqrt{\rho}b}{\kappa}, \quad D = E = -\frac{CL(\rho e^{-i\theta})}{X}A, \end{aligned}$$

which indicates that the five constants A, B, C, D , and E are in fact real valued.

In view of Eq. (5.2), we can rewrite Eq. (5.1) in the following form:

$$(5.3) \quad \begin{aligned} \phi_1(\xi) = & iA \left[2\mu\varpi_{21} - \frac{CL(\rho e^{-i\theta})\sigma_{12}^\infty}{X} \right] [K(\xi\sqrt{\rho}e^{i\theta}) + K(\xi\sqrt{\rho}e^{-i\theta})] \\ & + iC\sigma_{12}^\infty K(\xi\sqrt{\rho}) + F, \quad \rho \leq |\xi| \leq \frac{1}{\rho}. \end{aligned}$$

The other analytic function $\psi_1(\xi)$ can be obtained from the analytic continuation in Eq. (3.10) as:

$$(5.4) \quad \begin{aligned} \psi_1(\xi) = & 2i\mu\varpi_{21}\bar{\omega}\left(\frac{1}{\xi}\right) - i\sigma_{12}^\infty\omega(\xi) + \kappa\bar{\phi}_1\left(\frac{1}{\xi}\right) \\ & - \bar{\omega}\left(\frac{1}{\xi}\right) \frac{\phi_1'(\xi)}{\omega'(\xi)} - \bar{\gamma}, \quad \rho \leq |\xi| \leq 1. \end{aligned}$$

The resultant moment about the origin on the non-circular boundary L_1 should be zero. This condition results in

$$(5.5) \quad \operatorname{Re} \left\{ \int_{|\xi|=1} \psi_1(\xi) \omega'(\xi) d\xi \right\} = 0.$$

By substituting Eqs. (5.4) into Eq. (5.5) and making the use of Eq. (5.3), we finally obtain

$$(5.6) \quad \frac{\varpi_{21}}{\varepsilon_{12}^\infty} = \frac{C(\kappa + 1) \left[\frac{AI_2 L(\rho e^{-i\theta})}{X} - I_3 \right]}{2I_1 + AI_2(\kappa + 1)},$$

where

$$(5.7) \quad \varepsilon_{12}^\infty = \frac{\sigma_{12}^\infty}{2\mu},$$

and

$$(5.8) \quad \begin{aligned} I_1 &= -\frac{1}{2} \operatorname{Im} \left\{ \int_{|\xi|=1} \overline{\omega(\xi)} \omega'(\xi) d\xi \right\}, \\ I_2 &= \operatorname{Im} \left\{ \int_{|\xi|=1} [\overline{K(\xi \sqrt{\rho} e^{i\theta})} + \overline{K(\xi \sqrt{\rho} e^{-i\theta})}] \omega'(\xi) d\xi \right\}, \\ I_3 &= \operatorname{Im} \left\{ \int_{|\xi|=1} \overline{K(\xi \sqrt{\rho})} \omega'(\xi) d\xi \right\}. \end{aligned}$$

In Eq. (5.8), I_1 is the area of each non-circular inhomogeneity. Once the three regular integrals in Eq. (5.8) are evaluated by the trapezoidal rule [3], the rigid body rotation of each rigid inhomogeneity can be determined from Eq. (5.6). We illustrate in Fig. 3 the calculated $\varpi_{21}/\varepsilon_{12}^\infty$ for different values of ρ and κ . It is seen from Fig. 3 that: (i) the magnitude of $\varpi_{21}/\varepsilon_{12}^\infty$ decreases as ρ increases and/or κ increases (Poisson's ratio decreases); (ii) as $\rho \rightarrow 0$ for two rigid elliptical inhomogeneities elongated in the x_2 -direction each with an aspect ratio of 1/3 set far apart from each other, $\varpi_{21}/\varepsilon_{12}^\infty = m(\kappa + 1)/(\kappa + m^2)$ with $m = -0.5$, which is in agreement with the result for an isolated rigid elliptical inhomogeneity under remote shear [6–8]; (iii) as $\rho \rightarrow 1$ (the circumscribed boundary tends to a circle), $\varpi_{21}/\varepsilon_{12}^\infty = 0$ as expected (a rigid circular inhomogeneity will not undergo any rigid body rotation under any remote stress).

Substituting Eq. (5.3) into Eq. (3.9) and using the property in Eq. (4.6), we arrive at the constant γ as

$$(5.9) \quad \gamma = i\kappa A \left[2\mu \varpi_{21} - \frac{CL(\rho e^{-i\theta}) \sigma_{12}^\infty}{X} \right] + \frac{i\kappa C \sigma_{12}^\infty}{2},$$

which indicates that γ is purely imaginary.

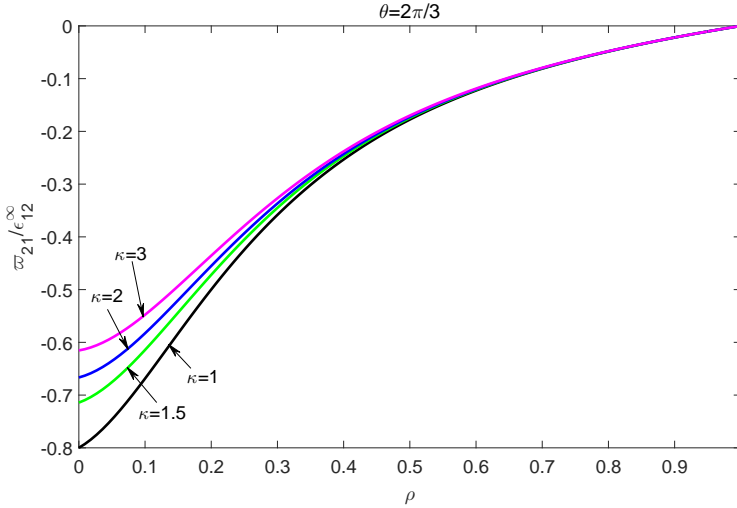


FIG. 3. Variations of $\varpi_{21}/\varepsilon_{12}^\infty$ as a function of ρ and κ with $\theta = 2\pi/3$.

Using Eq. (5.3) to enforce the condition in Eq. (4.8), we arrive at the constant F as

$$\begin{aligned}
 (5.10) \quad F &= -iA \left[2\mu\varpi_{21} - \frac{CL(\rho e^{-i\theta})\sigma_{12}^\infty}{X} \right] [K(-\rho e^{i\theta}) + K(-\rho e^{-i\theta})] \\
 &\quad - iC\sigma_{12}^\infty K(-\rho) \\
 &= -iC\sigma_{12}^\infty K(-\rho),
 \end{aligned}$$

which indicates that F is purely imaginary.

Now the pair of analytic functions in Eqs. (5.3) and (5.4) has been completely determined. The elastic field of stresses and displacements in the matrix due to the remote shear stress σ_{12}^∞ is now found by substituting Eqs. (5.3) and (5.4) into Eq. (3.4) and the subsequent results into Eqs. (2.1) and (2.2).

6. Remote behaviors of $\phi_1(z)$ and $\psi_1(z)$

When subjected to uniform remote normal stresses σ_{11}^∞ and σ_{22}^∞ , the remote asymptotic behaviors of $\phi_1(z)$ and $\psi_1(z)$ can be derived as:

$$(6.1) \quad \phi_1(z) \cong \frac{\lambda_1}{z} + O\left(\frac{1}{z^2}\right), \quad \psi_1(z) \cong \frac{\lambda_2}{z} + O\left(\frac{1}{z^2}\right), \quad |z| \rightarrow \infty,$$

where λ_1 and λ_2 are two real numbers given by:

$$\begin{aligned}
 \lambda_1 = \bar{\lambda}_1 &= -\frac{1}{\pi} \operatorname{Im} \left\{ \int_{|\xi|=1} \phi_1(\xi) \omega'(\xi) d\xi \right\} \\
 &= \frac{AI_4}{4\pi} \left[(\kappa - 1)(\sigma_{11}^\infty + \sigma_{22}^\infty) - \frac{2CL(\rho e^{-i\theta})(\sigma_{11}^\infty - \sigma_{22}^\infty)}{X} \right] \\
 &\quad + \frac{CI_5(\sigma_{22}^\infty - \sigma_{11}^\infty)}{2\pi}, \\
 (6.2) \quad \lambda_2 = \bar{\lambda}_2 &= -\frac{1}{\pi} \operatorname{Im} \left\{ \int_{|\xi|=1} \psi_1(\xi) \omega'(\xi) d\xi \right\} \\
 &= \frac{\kappa - 1}{2\pi} \left\{ I_1(\sigma_{11}^\infty + \sigma_{22}^\infty) \right. \\
 &\quad + AI_2 \left[\frac{(\kappa - 1)(\sigma_{11}^\infty + \sigma_{22}^\infty)}{2} - \frac{CL(\rho e^{-i\theta})(\sigma_{11}^\infty - \sigma_{22}^\infty)}{X} \right] \\
 &\quad \left. + CI_3(\sigma_{22}^\infty - \sigma_{11}^\infty) \right\},
 \end{aligned}$$

where the real constants A and C are given by Eq. (4.3), I_1 , I_2 and I_3 are determined by Eq. (5.8), and the two real constants I_4 and I_5 are determined by the following two integrals:

$$\begin{aligned}
 I_4 &= \operatorname{Im} \left\{ \int_{|\xi|=1} [K(\xi\sqrt{\rho}e^{i\theta}) + K(\xi\sqrt{\rho}e^{-i\theta})] \omega'(\xi) d\xi \right\}, \\
 (6.3) \quad I_5 &= \operatorname{Im} \left\{ \int_{|\xi|=1} K(\xi\sqrt{\rho}) \omega'(\xi) d\xi \right\}.
 \end{aligned}$$

When subjected to the uniform remote shear stress σ_{12}^∞ , the remote asymptotic behaviors of $\phi_1(z)$ and $\psi_1(z)$ are derived as:

$$(6.4) \quad \phi_1(z) \cong \frac{i\lambda_3}{z} + O\left(\frac{1}{z^2}\right), \quad \psi_1(z) \cong O\left(\frac{1}{z^2}\right), \quad |z| \rightarrow \infty,$$

where λ_3 is a real number given by

$$\begin{aligned}
 (6.5) \quad \lambda_3 = \bar{\lambda}_3 &= \frac{1}{\pi} \int_{|\xi|=1} \phi_1(\xi) \omega'(\xi) d\xi \\
 &= -\frac{AI_4}{\pi} \left[2\mu\varpi_{21} - \frac{CL(\rho e^{-i\theta})\sigma_{12}^\infty}{X} \right] - \frac{CI_5\sigma_{12}^\infty}{\pi},
 \end{aligned}$$

with the real constants A and C given by Eq. (5.2).

We need to evaluate the two regular integrals in Eq. (6.3) in addition to the three regular integrals in Eq. (5.8) to identify the remote asymptotic behaviors of $\phi_1(z)$ and $\psi_1(z)$. We illustrate in Figs. 4 and 5 the remote asymptotic behaviors of $\phi_1(z)$ and $\psi_1(z)$ under uniform remote normal stresses. The results in Figs. 4 and 5 as $\rho \rightarrow 1$ agree with those for a rigid circular inhomogeneity [5]. The results

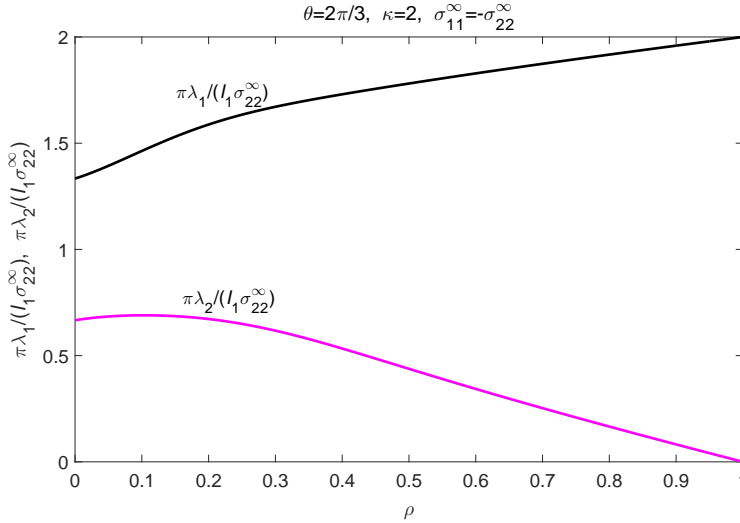


FIG. 4. Variations of $\pi\lambda_1/(I_1\sigma_{22}^\infty)$ and $\pi\lambda_2/(I_1\sigma_{22}^\infty)$ as functions of ρ with $\theta = 2\pi/3$, $\kappa = 2$, $\sigma_{11}^\infty = -\sigma_{22}^\infty$.

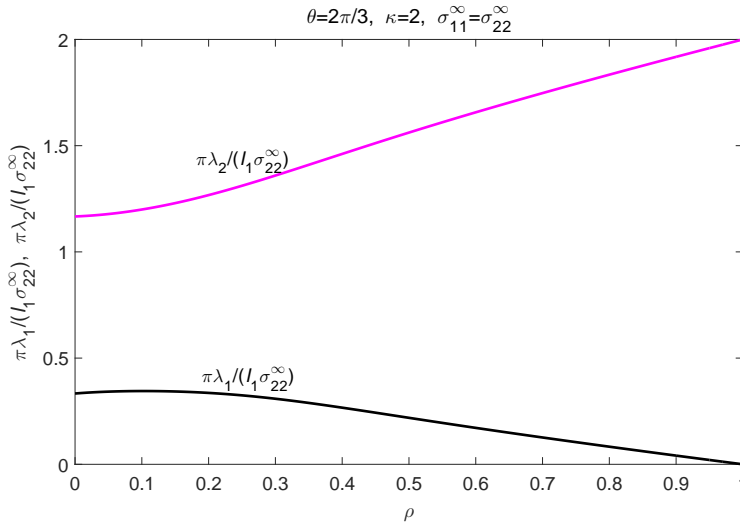


FIG. 5. Variations of $\pi\lambda_1/(I_1\sigma_{22}^\infty)$ and $\pi\lambda_2/(I_1\sigma_{22}^\infty)$ as functions of ρ with $\theta = 2\pi/3$, $\kappa = 2$, $\sigma_{11}^\infty = \sigma_{22}^\infty$.

in Figs. 4 and 5 as $\rho \rightarrow 0$ recover the following analytical solution derived previously for two rigid elliptical inhomogeneities elongated in the x_2 -direction with the major axis three times larger than the minor axis set far apart from each other

$$(6.6) \quad \begin{aligned} \frac{\pi \lambda_1}{I_1} &= \frac{\sigma_{22}^\infty(2+m-\kappa m) - \sigma_{11}^\infty(2-m+\kappa m)}{2\kappa(1-m^2)}, \\ \frac{\pi \lambda_2}{I_1} &= \frac{\sigma_{22}^\infty[m(2+m) - \kappa(1+m)^2 + \kappa^2] - \sigma_{11}^\infty[m(2-m) + \kappa(1-m)^2 - \kappa^2]}{2\kappa(1-m^2)}, \end{aligned}$$

where $m = -0.5$.

When $m = 0$ for a rigid circular inhomogeneity, Eq. (6.6) reduces to

$$(6.7) \quad \begin{aligned} \frac{\pi \lambda_1/2}{I_1/4} &= \frac{2(\sigma_{22}^\infty - \sigma_{11}^\infty)}{\kappa}, \\ \frac{\pi \lambda_2/2}{I_1/4} &= (\kappa - 1)(\sigma_{11}^\infty + \sigma_{22}^\infty), \end{aligned}$$

which are simply the results as $\rho \rightarrow 1$ in Figs. 4 and 5. Note that the area enclosed by L_1 is one quarter of that enclosed by the circumscribed boundary (a circle) while in Eq. (6.7) I_1 is the area of a circle.

The above asymptotic behaviors of $\phi_1(z)$ and $\psi_1(z)$ in Eqs. (6.1) and (6.4) are related to the compressibility and shear compliance of the two identical rigid non-circular inhomogeneities [5, 10–13].

It is further deduced from Eqs. (6.1) and (6.2) that $\phi_1(z) \cong O(z^{-2})$ as $|z| \rightarrow \infty$ when the following condition is met

$$(6.8) \quad \frac{\sigma_{11}^\infty}{\sigma_{22}^\infty} = \frac{AI_4(\kappa - 1) + 2CI_5 + \frac{2ACI_4L(\rho e^{-i\theta})}{X}}{-AI_4(\kappa - 1) + 2CI_5 + \frac{2ACI_4L(\rho e^{-i\theta})}{X}}.$$

Also, $\sigma_{11} + \sigma_{22} \cong \sigma_{11}^\infty + \sigma_{22}^\infty + O(|z|^{-3})$ as $|z| \rightarrow \infty$ when the loading ratio $\sigma_{11}^\infty/\sigma_{22}^\infty$ is chosen according to Eq. (6.8), implying that the mean stress within the matrix is almost undisturbed. Thus, the two rigid inhomogeneities are weakly harmonic. We illustrate in Fig. 6 the loading ratio $\sigma_{11}^\infty/\sigma_{22}^\infty$ for different values of ρ and κ determined by Eq. (6.8). It is seen from Fig. 6 that: (i) $\sigma_{11}^\infty/\sigma_{22}^\infty$ is a decreasing function of ρ and an increasing function of κ ; (ii) as $\rho \rightarrow 0$ for two rigid elliptical inhomogeneities elongated in the x_2 -direction each with an aspect ratio of 1/3 set far apart from each other, $\sigma_{11}^\infty/\sigma_{22}^\infty = (3 + \kappa)/(5 - \kappa)$, which is in agreement with the result for an isolated harmonic rigid elliptical inhomogeneity [14] and which is also the result by setting $\lambda_1 = 0$ in Eq. (6.6)₁; (iii) $\sigma_{11}^\infty/\sigma_{22}^\infty = 1$ as $\rho \rightarrow 1$, which is just the result for a harmonic rigid circular inhomogeneity.

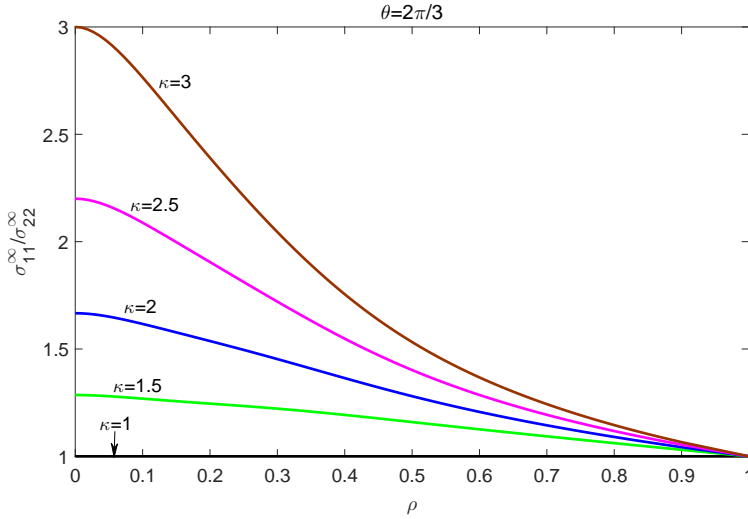


FIG. 6. Variations of $\sigma_{11}^\infty/\sigma_{22}^\infty$ as a function of ρ and κ determined by Eq. (6.8) with $\theta = 2\pi/3$.

7. Conclusions

We have solved analytically the plane elasticity problem of two identical rigid non-circular inhomogeneities in an infinite elastic matrix under uniform remote normal and shear stresses. The pair of analytic functions $\phi_1(\xi)$ and $\psi_1(\xi)$ due to remote normal stresses is obtained in Eqs. (4.5) and (4.10) and that due to remote shear stress in Eqs. (5.3) and (5.4) following the introduction of the conformal mapping function in Eq. (3.1). By imposing the balance of moments around each rigid inhomogeneity, the rigid body rotation of each rigid inhomogeneity induced by the remote shear stress is determined by Eq. (5.6) in which the three regular integrals in Eq. (5.8) are evaluated using the trapezoidal rule. The remote asymptotic behaviors of $\phi_1(z)$ and $\psi_1(z)$ are determined by Eqs. (6.1) and (6.4) containing two new integrals in Eq. (6.3) in addition to the three integrals in Eq. (5.8).

The two rigid non-circular inhomogeneities studied in this paper can be viewed as two elastic inhomogeneities whose shear moduli approach infinity. The two non-circular traction-free pores studied in [3] can be viewed as two elastic inhomogeneities whose shear moduli approach zero such that their compressibilities approach infinity. The case of two non-circular incompressible liquid inclusions, as a special case of [4], can be viewed as that of two elastic inhomogeneities whose shear moduli approach zero while their Poisson's ratios approach the value of $1/2$ in a specific way compatible with their compressibilities approaching zero [15].

The method based on Laurent series expansion can be used to solve the plane elasticity problem of two rigid circular inhomogeneities under uniform remote

in-plane stresses. It is then required to solve a set of coupled linear algebraic equations to identify the coefficients appearing in the Laurent series expansion and the rigid body rotations of the two rigid circular inhomogeneities. In this case, however, the solution method based on the Schottky–Klein prime function used in this paper becomes invalid since the doubly connected domain occupied by the matrix is not a quadrature domain.

Acknowledgments

This work is supported by a Discovery Grant from the Natural Sciences and Engineering Research Council of Canada (Grant No: RGPIN-2023-03227 Schiavo).

References

1. N.I. MUSKHELISHVILI, *Some Basic Problems of the Mathematical Theory of Elasticity*, P. Noordhoff, Groningen, 1953.
2. A.H. ENGLAND, *Complex Variable Method in Elasticity*, John Wiley and Sons, New York, 1971.
3. D. CROWDY, *Stress fields around two pores in an elastic body: exact quadrature domain solutions*, Proceedings of the Royal Society A, **471**, 2180, 20150240, 2015.
4. X. WANG, P. SCHIAVONE, *Two non-circular compressible liquid inclusions in an infinite elastic matrix*, Zeitschrift für Angewandte Mathematik und Mechanik, **105**, 2, e202401292, 2025.
5. I. JASIUK, *Cavities vis-a-vis rigid inclusions: Elastic moduli of materials with polygonal inclusions*, International Journal of Solids and Structures, **32**, 407–422, 1995.
6. X. WANG, E. PAN, L.J. SUDAK, *Uniform stresses inside an elliptical inhomogeneity with an imperfect interface in plane elasticity*, The American Society of Mechanical Engineers (ASME) Journal of Applied Mechanics, **75**, 054501, 2008.
7. X. WANG, P. SCHIAVONE, *Uniform in-plane stresses and strains inside an incompressible nonlinear elastic elliptical inhomogeneity*, European Journal of Mechanics A/Solids, **102**, 105085, 2023.
8. X. WANG, P. SCHIAVONE, *A partially debonded rigid elliptical inclusion with a liquid slit inclusion occupying the debonded portion*, Mathematics and Mechanics of Solids, **29**, 11, 2224–2235, 2024.
9. T.C.T. TING, *Anisotropic Elasticity: Theory and Applications*, Oxford University Press, New York, 1996.
10. I. JASIUK, J. CHEN, M.F. THORPE, *Elastic moduli of two dimensional materials with polygonal and elliptical holes*, Applied Mechanics Review, **47**, Suppl. 1, 18–21, 1994.
11. T.C. EKNELIGODA, R.W. ZIMMERMAN, *Compressibility of two-dimensional pores having N-fold axes of symmetry*, Proceedings of the Royal Society of London A, **462**, 1933–1947, 2006.

12. T.C. EKNELIGODA, R.W. ZIMMERMAN, *Shear compliance of two-dimensional pores possessing N -fold axis of rotational symmetry*, Proceedings of the Royal Society of London A, **464**, 759–775, 2008.
13. T.C. EKNELIGODA, R.W. ZIMMERMAN, *Boundary perturbation solution for nearly circular holes and rigid inclusions in an infinite elastic medium*, Journal of Applied Mechanics, **75**, 1, 148–155, 2008.
14. G.S. BJORKMAN, *Design of pressure vessel pads and attachments to minimize global stress concentrations*, Transactions, Structural Mechanics in Reactor Technology (SMiRT), **19**, Toronto, August 2007.
15. J. WU, C.Q. RU, L. ZHANG, *An elliptical liquid inclusion in an infinite elastic plane*, Proceedings of the Royal Society A, **474**, 2215, 20170813, 2018.

Received January 2, 2025; revised version April 7, 2025.

Published online June 2, 2025.
